Experimental Study on Reinforcement of Existing Bridge Pile Foundations Subjected to Lowering of Riverbed Soil Using Sheet Pile Wall

Tanatan TIKANTA
Civil engineer, Department of Rural Roads, the Ministry of Transportation, Chiang Mai, Thailand
Tatsunori MATSUMOTO
Professor, Graduate School of Kanazawa University, Kanazawa, Japan
Email: matsumoto@se.kanazawa-u.ac.jp
Anh-Tuan VU
Lecturer, Department of Civil Engineering, Le Quy Don Technical University, Hanoi, Vietnam
Shinya SHIMONO
Technician, Kanazawa University, Kanazawa, Japan

ABSTRACT

Development of an effective countermeasure for the existing bridge foundations subjected to the influence of riverbed excavation in Thailand is the main objective of this study. Due to the riverbed soil excavation for the utilization in construction works for many years, the levels of riverbed have been considerably decreased, resulting in reduction of embedded lengths of piles for bridge foundations. The reductions of pile embedment lengths, in other words, reductions of bearing capacity due to the lowering of riverbed soil is the main cause of bridge pile foundation settlements or collapses at present. In order to prevent the damages of existing bridge pile foundations caused by riverbed soil excavation, a reinforcement method using sheet piles called “Sheet Pile Wall (SPW) reinforcement” is proposed in this paper. The proposed SPW reinforcement method consists of 2 simple steps without new additional piles or any modifications of existing structures. Firstly, sheet piles are constructed surrounding the existing problematic bridge pile foundation. Secondly, the empty space inside the SPW is filled with sand or other porous materials such as crushed concrete. In order to investigate the performance of the proposed SPW reinforcement method, series of load tests on the small sized model single pile and model 4-pile pile foundation were carried out. The experimental results show that the proposed SPW reinforcement method is very efficient and promising.

Key words: *Reinforcement, Existing bridge, Pile foundation, Riverbed soil excavation, Model load test*

1. Introduction

In the past decade, the Mae Nam Ping River crossing bridges in Chiang Mai and Lamphun, located in the northern area of Thailand (**Fig. 1**), encountered pile foundation damages frequently.

Fig. 2 shows the first case of bridge foundation damage in 2006. One of pile foundations of the bridge LP.010 in Lamphun settled during a high flood season. The investigation and arrangement for the solution were performed for 2 years. The settled bridge LP.010 was repaired in 2008 by using new additional piles, extending the footing, jacking up the bridge girders and extending the height of the settled bridge pier by 0.80 m to keep smooth on the bridge slabs as shown in **Fig. 3**.

A few years later, another pile foundation at the pier No.7 of the same bridge LP.010 settled again during a high flood season in 2010. This time, the settled pile foundation collapsed and fell down into the river within 5 days after the settlement. The collapsed bridge LP.010 was repaired in 2013 by constructions of two new pile foundations at new locations on both sides of the previously collapsed foundation.

Fig. 1 Location of the Mae Nam Ping River in Chiang Mai and Lamphun, Thailand

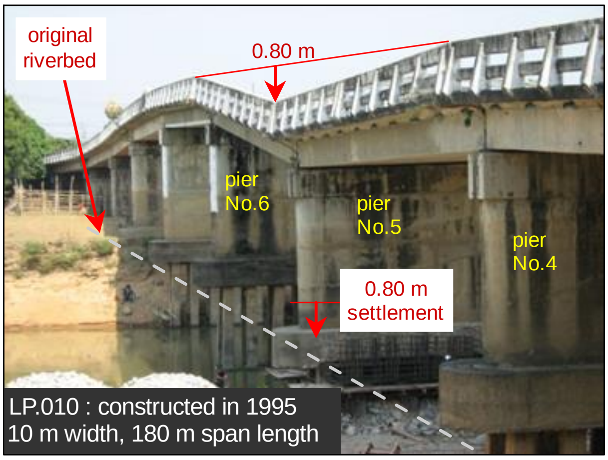

Fig. 2 Differential settlement of the bridge LP.010 in Lamphun, Thailand (2006)

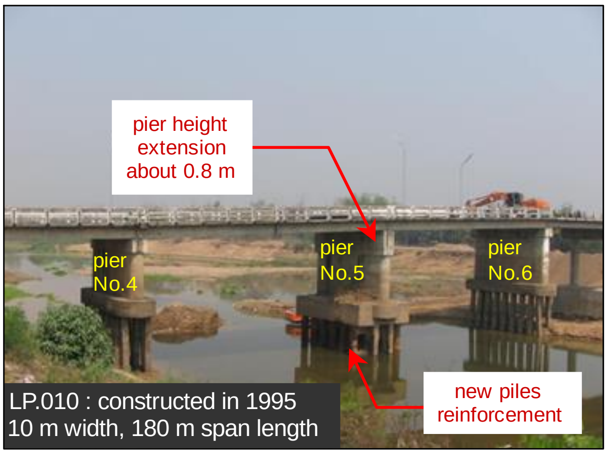

Fig. 3 Repair of the settled bridge LP.010 in Lamphun, Thailand (2008)

In the same year of 2010, two other bridges crossing the Mae Nam Ping River named CM.015 and CM.025 also encountered the differential settlement problem. Both of them were repaired in 2013 by the similar way as the repair of the previous settled bridge (LP.010) in 2008.

The main cause of the bridge foundation damages mentioned above was the lowering of riverbed soil, in other words, the reduction of pile embedment length. Though the damaged bridges were repaired, most of undamaged bridge pile foundations along the river still have potential risks of being damaged due to the riverbed soil excavation as shown in **Fig. 4**.

Although the repairs of the damaged bridge were successful, the repair method could not be applied to the reinforcement of undamaged bridge foundations, because of a high cost and a long construction time of the repair method in which additional piles and extension of footing were required. Hence, in order to obtain an efficient countermeasure for the existing bridge pile foundations subjected to the problem of riverbed soil excavation, a fundamental experimental study was carried out in this paper. Considering safety, economic and uncomplicated approach, a reinforcing method using sheet pile wall (SPW) called "SPW reinforcement" is proposed in this study.

Fig. 4 An example case of undamaged bridge which has potential risk of being damaged (2012)

Fig. 5 illustrates the concept of the SPW reinforcement method. The construction procedure of the SPW reinforcement consists of two simple steps without new additional piles or any modifications of existing structures. Firstly, a sheet pile wall is constructed surrounding the existing problematic bridge pile foundation. Finally, the empty space inside the SPW is filled with sand or other porous materials such as crushed concrete.

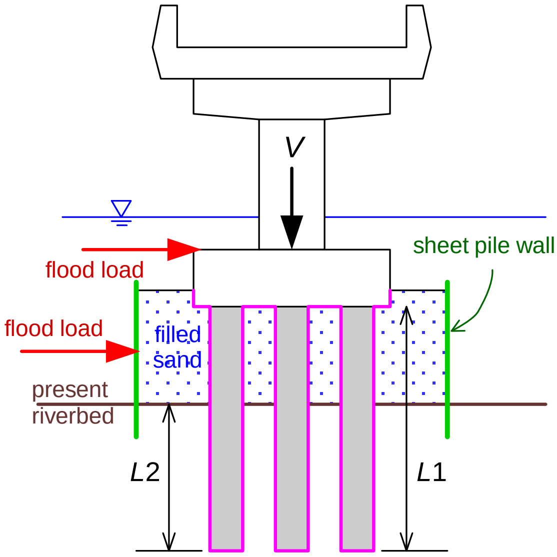

Fig. 5 The concept of Sheet Pile Wall (SPW) reinforcement method

A method for reinforcing an existing pile foundation by means of sheet pile wall, called the In-cap Method, has been proposed by Fukuda et al. (2005). The In-cap method surrounds the existing foundation footing to a required depth, solidifies the inside of the sheet piles for improvement of the footing and integrates the improved footing with the existing foundation.

The SPW reinforcement method proposed in this paper has similar feature to the In-cap Method, however, a big difference between the two methods is that there is no soil (ground) around the sheet pile wall in the SPW reinforcement method. Hence, investigation of the reinforcement mechanisms in the SPW method was carried out in this research.

2. Experimental models

In order to validate the performance of SPW reinforcement method, series of model load tests on a single pile and 4-pile pile foundation were carried out.

2.1. Model piles and model 4-pile pile foundation

An aluminum pipe of 32 mm in diameter and 600 mm in length as shown in **Fig. 6** was employed as a model pile in the single pile load tests. Strain gauges were instrumented along the pile shaft to obtain axial forces, shear forces and bending moments during the load tests. Sand particles of the sand used for the model ground were glued on the pile shaft to increase shaft friction and to protect strain gauges from damage. An end cap was not attached to the pile tip so that the pile had open-ended condition. Physical and mechanical properties of the model single pile are listed in **Table 1**.

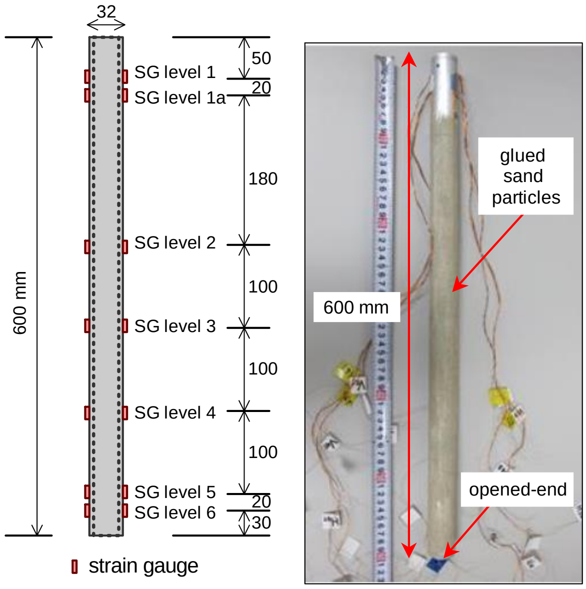

Fig. 6 Configurations of the model pile for single pile load tests

Table 1. Physical and mechanical properties of the model single pile

Type of material	Aluminium alloy JIS A6063
Pile length, L_p (mm)	600
Outer diameter, D_o (mm)	32
Inner diameter, D_i (mm)	29.3
Wall thickness, t_w (mm)	1.35
Density, ρ_p (g/cm^3)	2.70
Young's modulus, E_p (MPa)	65,400
Poisson's ratio, ν_p	0.33

Aluminum pipes of 20 mm in diameter and 285 mm in length as shown in **Fig. 7** were employed as model piles in a 4-pile pile foundation model. Each model pile was instrumented with strain gauges and was glued with sand particles as similar to the model single pile.

An end cap was attached to the pile tip so that the pile had close-ended condition. Physical and mechanical properties of the model piles are listed in **Table 2**.

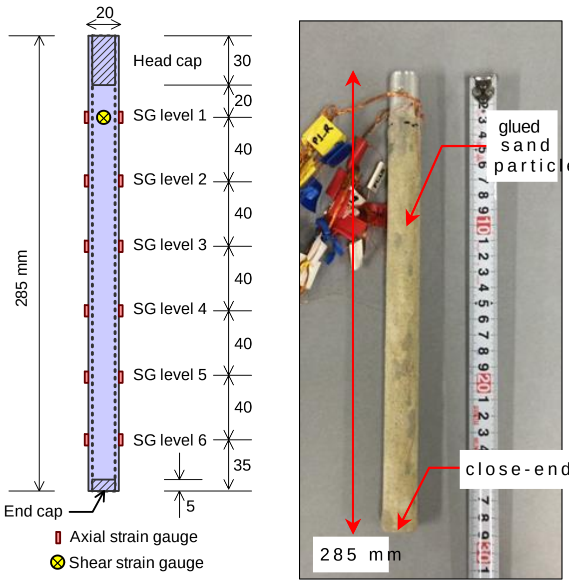

Fig. 7 Configurations of the model piles consisted in the 4-pile pile foundation

Table 2. Physical and mechanical properties of the model piles consisted in the 4-pile pile foundation

Type of material	Aluminium alloy JIS A6063
Pile length, L (mm)	285
Outer diameter, D_o (mm)	20
Inner diameter, D_i (mm)	17.8
Wall thickness, t (mm)	1.1
Density, ρ (g/cm^3)	2.70
Young's modulus, E (MPa)	65,000
Poisson's ratio, ν	0.33

Fig. 8 shows the configurations and dimensions of the 4-pile pile foundation. The pile cap or raft was made of aluminium alloy JIS A2017 that had physical and mechanical properties as listed in **Table 3**.

2.2. Model ground

The sand that has physical and mechanical properties listed in **Table 4** was used as the model ground throughout the experiments. The model single pile and the model 4-pile pile foundation were set in the model ground of dry sand which was prepared in a cylindrical model ground container as shown in **Fig. 9**.

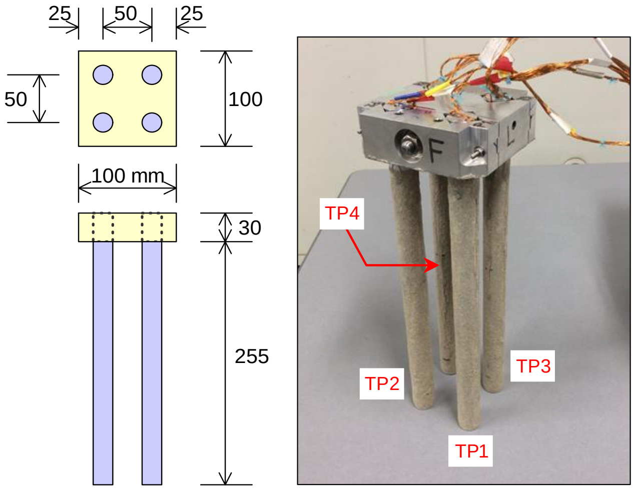

Fig. 8 Configurations of the 4-pile pile foundation

Table 3. Physical and mechanical properties of the model pile cap used in the 4-pile pile foundation

Type of material	Aluminium alloy
Width, B (mm)	100
Length, L (mm)	100
Thickness, t (mm)	30
Pile spacing, s (mm)	50
Normalised pile spacing, s/D	2.5
Density, ρ (g/cm^3)	2.79
Young's modulus, E (MPa)	73,000
Poisson's ratio, ν	0.33

Table 4. Properties of the sand used as model ground

Soil particle density, ρ_s (g/cm^3)	2.668
Minimum dry density, ρ_{dmin} (g/cm^3)	1.269
Maximum dry density, ρ_{dmax} (g/cm^3)	1.604
Maximum void ratio, e_{max}	1.103
Minimum void ratio, e_{min}	0.663
Cohesion, c' (kPa)	0
Internal friction angle, ϕ' (degree)	42.8
Poisson's ratio, ν	0.30
Model ground density, ρ (g/cm^3)	1.524
Model ground relative density, D_r (%)	80

2.3. Model sheet pile walls (SPW)

A PVC (polyvinyl chloride) pipe of 140 mm in inner diameter and 135 mm in length as shown in **Fig. 10** was employed as the model SPW1 in the reinforcement stage of 4-pile pile foundation load tests. Strain gauges were instrumented on the outer surface of SPW1 to measure vertical (axial) and horizontal (hoop) strains during load tests. Geometrical and mechanical properties of the model SPW1 are listed in **Table 5**.

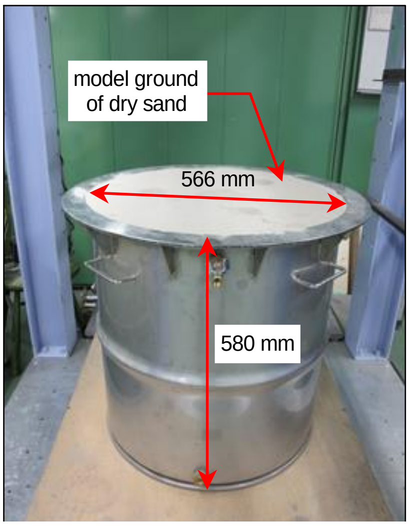

Fig. 9 Configurations of the cylindrical model ground container

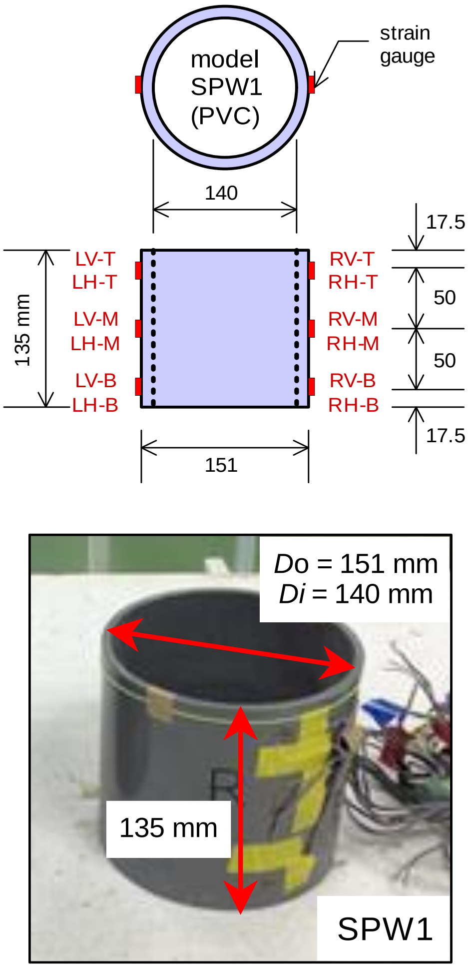

Fig. 10 Configurations of the model SPW1

Table 5. Properties of the model SPW1

Type of material	PVC
Outer diameter, D_o (mm)	151
Inner diameter, D_i (mm)	140
Height, H (mm)	135
Wall thickness, t (mm)	5.5
Density, ρ (g/cm^3)	1.415
Young's modulus, E (MPa)	2,100
Poisson's ratio, ν	0.31

The model SPW2 made of PVC pipe of 131 mm in inner diameter and 250 mm in length as shown in **Fig. 11** was employed in the reinforcement stage of the single pile load tests. The outer surface was instrumented with strain gauges similar to the model SPW1. Geometrical and mechanical properties of the model SPW2 are listed in **Table 6**.

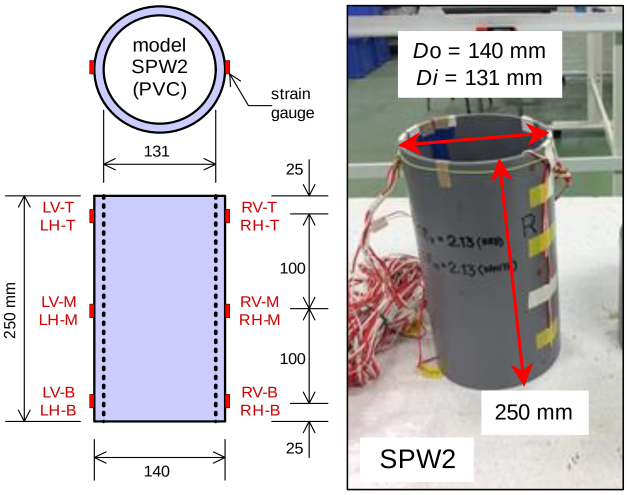

Fig. 11 Configurations of the model SPW2

Table 6. Properties of the model SPW2

Type of material	PVC
Outer diameter, D_o (mm)	140
Inner diameter, D_i (mm)	131
Height, H (mm)	250
Wall thickness, t (mm)	4.5
Density, ρ (g/cm^3)	1.415
Young's modulus, E (MPa)	1,900
Poisson's ratio, ν	0.20

3. Experimental results

3.1. Vertical load tests on the single pile

In series of vertical load tests (VLTs) on the single pile, VLTs in the initial stage, the embedment reduction stage (simulating riverbed soil excavation) and the reinforcement stage were carried out in the same model ground. The model pile was a kind of bored pile. First, the model ground of 180 mm in height was prepared, secondly the model pile was set on the model ground, and then the sand was poured around the model pile until the total height of the model ground reached 580 mm. In the embedment reduction stage, the top 50 mm ground was removed 4 times as shown in **Fig. 12** (steps No. 2 to No. 5). At step No. 5, the embedment length, L_d, was reduced to 200 mm from the initial embedment length of 400 mm. After the load test at step No.5, SPW2 (**Fig. 11**) was set on the ground surface.

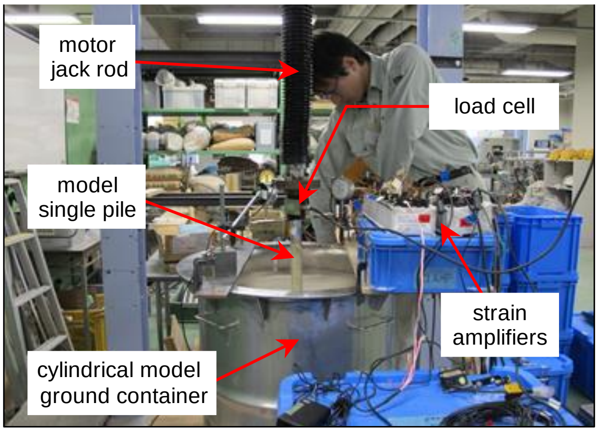

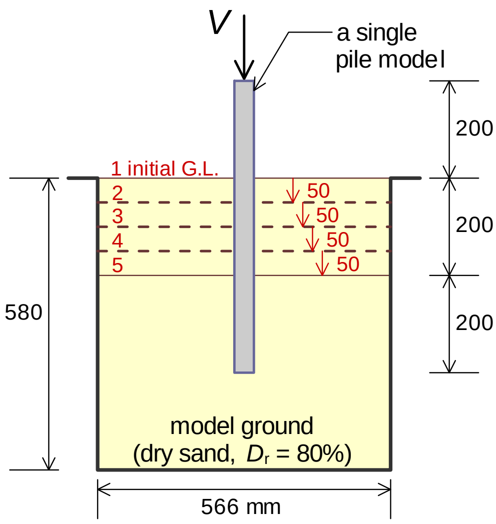

Fig. 12 Test conditions and sequences of VLTs on the single pile in the initial stage and the embedment reduction stage

In the reinforcement stage, the inside of SPW2 was refilled with the sand in 3 steps (No. 6 to No. 8) as shown in **Fig. 13**. In the step No. 8, the pile embedment length was recovered to that in the initial condition of 400 mm.

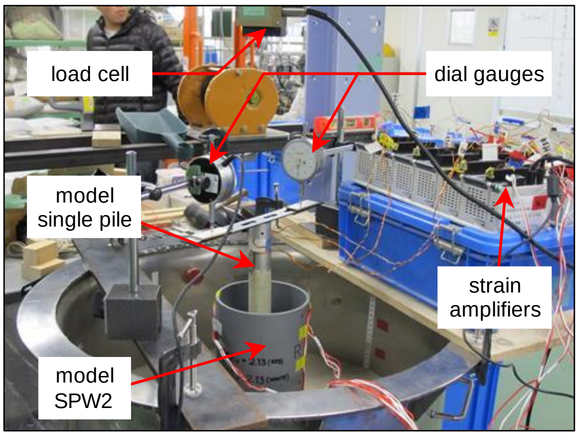

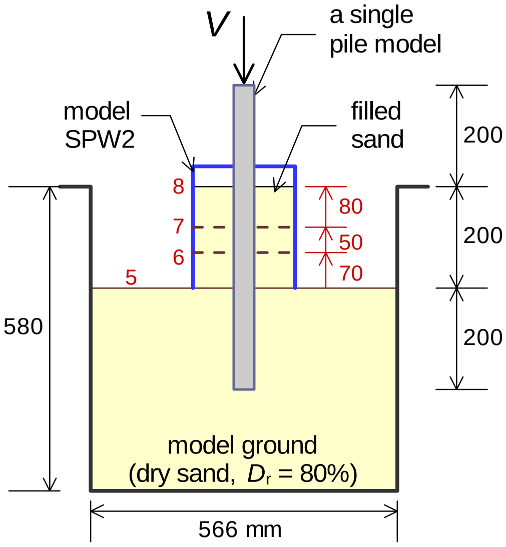

Fig. 13 Test conditions and sequences of VLTs on the single pile in the reinforcement stage

Fig. 14 shows load-settlement curves in the initial stage No. 1 and in the embedment reduction steps No. 2 to No. 5. It is seen that vertical resistances of the pile decreased with the reductions of pile embedment length from No. 1 to No. 5. Furthermore, though the pile embedment was remaining 50% in the final embedment reduction step No. 5, the yield resistance of about 900 N was less than 50% of the yield resistance exceeding 2,100 N in the initial stage No. 1.

Fig. 15 shows load-settlement curves in the final embedment reduction step No. 5 and in the reinforcement steps No. 6 to No. 8 comparing with the result in the initial stage No. 1.

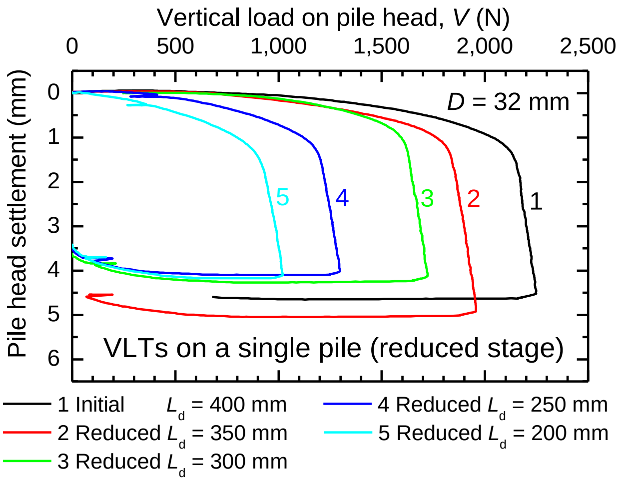

Fig. 14 Load-settlement curves of VLTs on the single pile in the initial stage and the embedment reduction stage

It is seen from **Fig. 15** that vertical resistance of the pile increased from No. 5 to No. 8 with increasing pile embedment length using the SPW reinforcement. At the final reinforcement step No. 8, the yield resistance of the pile recovered to about 70% of that in the initial stage No. 1 (or to about 140% of that in the final embedment reduction step No. 5).

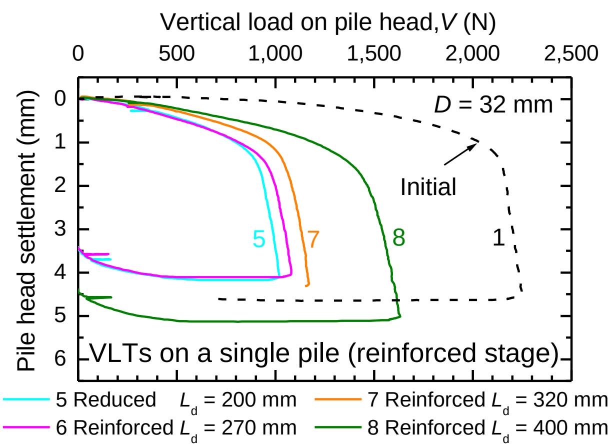

Fig. 15 Load-settlement curves of VLTs on the single pile in the reinforcement stage

Fig. 16 shows the axial force distributions of the pile (a) in the initial stage No.1, (b) in the final embedment reduction step No.5 and (c) in the final reinforcement step No. 8. It is seen from the comparison of **Fig. 16 (a)** and **(b)** that not only shaft friction resistance but also pile tip resistance in the final embedment reduction step No. 5 decreased compared with those of the initial stage No.1 due to the influence of pile embedment length reduction.

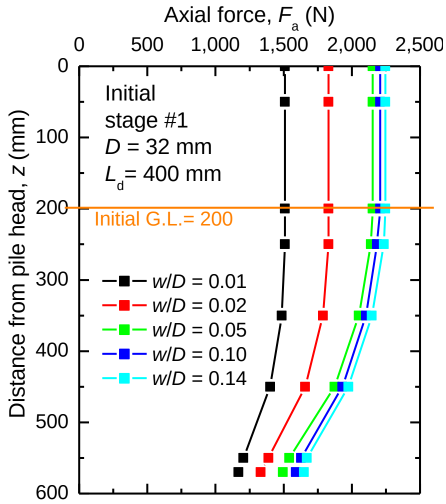

(a) in the initial stage No.1

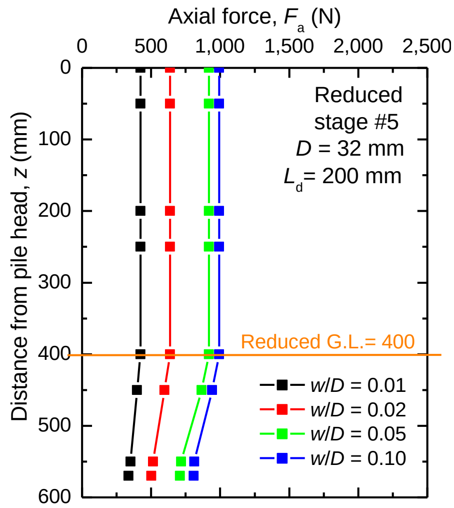

(b) in the final embedment reduction step No.5

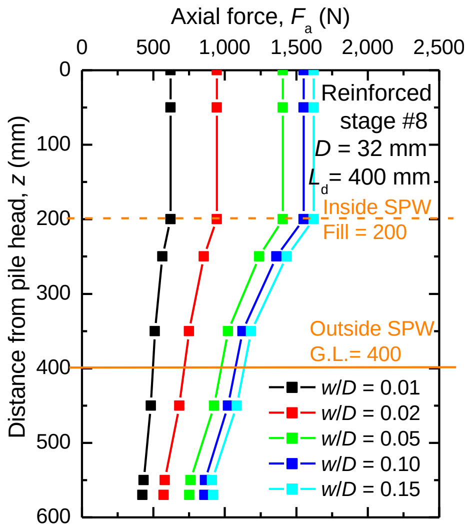

(c) in the final reinforcement step No. 8

Fig. 16 Axial force distributions of the single pile in VLTs

In the final reinforcement step No. 8 (**Fig. 16(c)**), the vertical resistance of the pile was improved due to the recovery of pile embedment length using the SPW reinforcement. However, the pile resistance in the final reinforcement step No. 8 was not fully recovered comparing with the results of the initial stage No.1 (**Fig. 16(a)**).

3.2. Vertical load tests on 4-pile pile foundation

In Sections 3.1, effectiveness of the SPW reinforcement was demonstrated. In order to investigate the effectiveness of the SPW reinforcement more in detail, vertical load tests on the 4-pile pile foundation model were carried out.

Similar to the VLTs on the single pile, VLTs on the 4-pile pile foundation were carried out in the initial condition and in each stage of the pile embedment length reduction and the SPW reinforcement, as shown in **Fig. 17** (reduction stage) and **Fig. 18** (reinforcement stage).

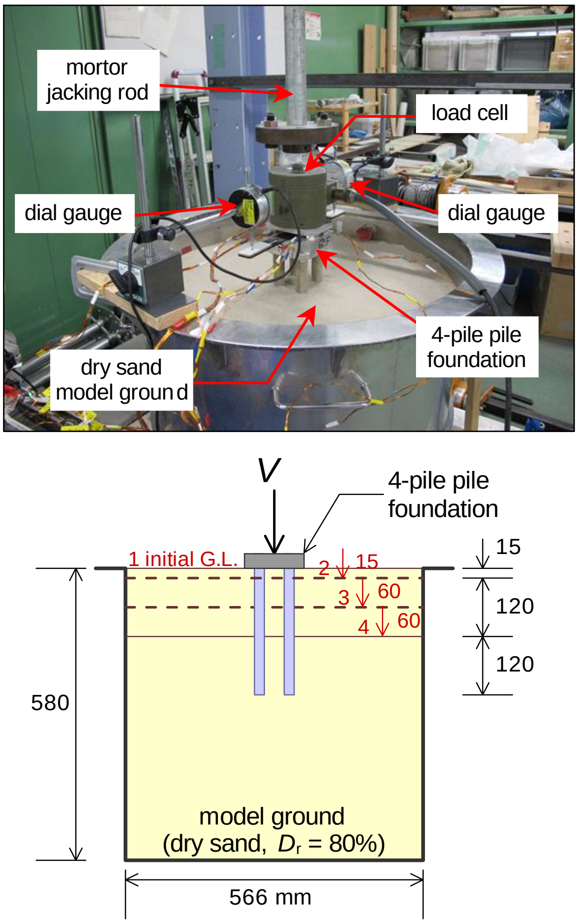

Fig. 17 Test conditions of VLTs on 4-pile pile foundation in the initial stage and the embedment reduction stage

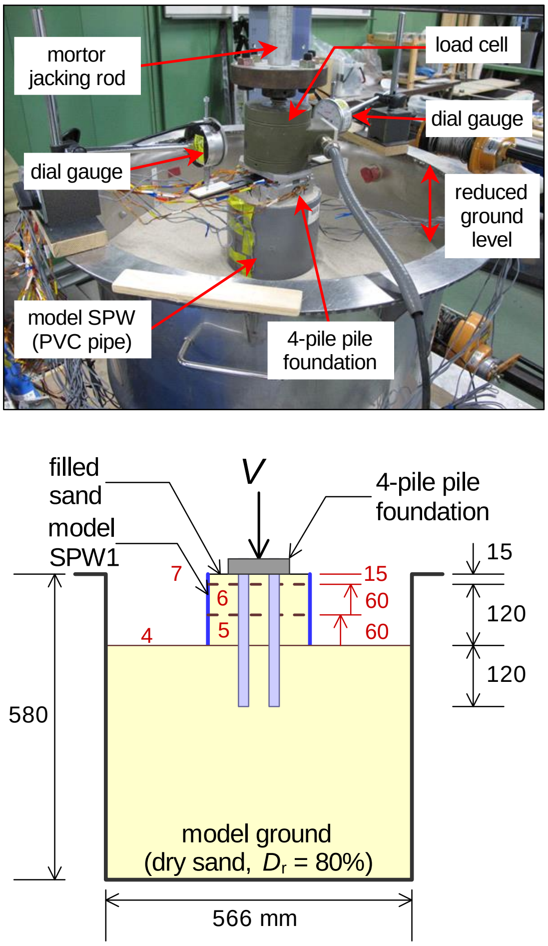

Fig. 18 Test conditions of VLTs on 4-pile pile foundation in the reinforcement stage

In the reinforcement stage, SPW1 was located very close to the model foundation, as shown in **Fig. 19**. It is desirable to minimize the size of the SPW so that the SPW structure does not interfere the river stream as much as possible when the SPW reinforcement is applied to an actual bridge foundation.

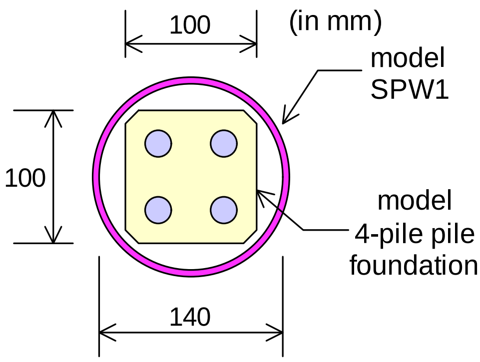

Fig. 19 Top view dimensions of SPW reinforcement in VLTs on 4-pile pile foundation

Fig. 20 shows load-settlement curves in the initial stage No.1 and the embedment reduction steps from No. 2 to No. 4. It is seen that vertical resistances and initial stiffness of the pile foundation decreased with the reductions of pile embedment length from No. 2 to No. 4. It is also seen that the load-settlement curves in the reduction steps No. 2 and No. 3 exhibit a plunging behaviour and the response in step No. 4 exhibits a softening behaviour, while the response in the initial stage No. 1 shows a progressive failure behaviour.

It is interesting to notice that the load-settlement behaviour in the stage No. 1 is different from those in the other stages. The initial stiffness of the load-settlement curve at the stage No. 1 is much higher than those in the other stage, and the pile at the stage No. 1 has higher resistance at larger settlements.

A reason for these results is attributed to the existence of the raft resistance in the stage No. 1. A part of the vertical load is transferred to the soil beneath the raft base, resulting in the increase of stress level and the stiffness of the soil. Although the figure is not shown, the shaft resistance of the piles in the stage No. 1 was larger than those in the other stages. This fact increases the initial stiffness of the load-settlement curve at the stage No. 1. At larger settlements, the raft resistance was mobilised larger, resulting in the larger total vertical resistance of the foundation in the stage No. 1.

It is also noted that the tangent stiffness at the stage No. 1 when *w* was around 0.5 mm was smaller than those in the other steps (No. 2 to 4). A reason may be the difference in the base stiffness of the pile. The base stiffness would have been lower at the stage No. 1 because the pile was in a bored state in case 1 and was in jacked state in No. 2 to 4 due to the penetration of the pile in the previous load test.

Fig. 21 shows load-settlement curves in the reinforcement steps from No.5 to No.7, comparing with the results in the final embedment reduction step No.4 and the initial stage No. 1. It is seen that the vertical resistances and stiffness of the 4-pile pile foundation increased from step No. 4 to step No. 7 with increasing pile embedment length using the SPW reinforcement. In particular, the vertical resistance in the final reinforcement step No. 7 was much greater than that of the initial stage No. 1.

Figs. 22 and **23** show changes of distributions of hoop strains and axial strains of the SPW with increasing normalised settlement of the foundation, *w*/*D*, where *w* is the settlement and *D* is the pile diameter, respectively, during load test in the final reinforcement step No. 7. Note that compression strain is taken as positive and tension strain is taken as negative. It is seen that the maximum values of both hoop strain and axial strain were generated around the SPW base.

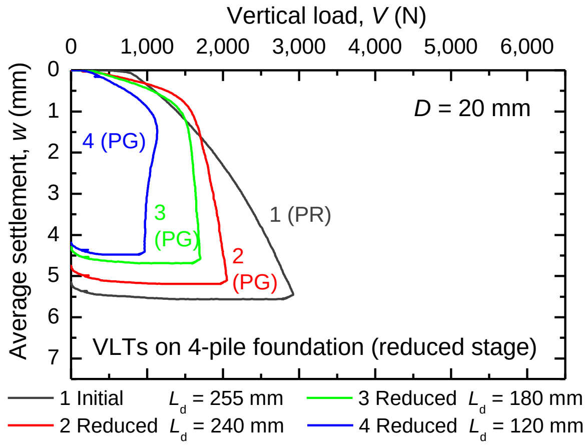

Fig. 20 Load-settlement curves of VLTs on 4-pile pile foundation in the initial stage and the stage of pile embedment reduction

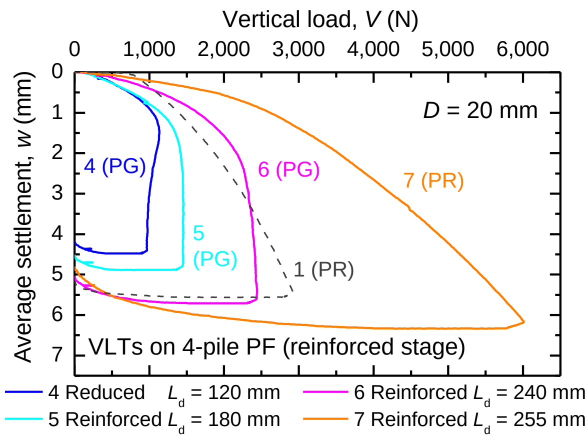

Fig. 21 Load-settlement curves of VLTs on 4-pile pile foundation in the reinforcement stage

It is also seen that absolute magnitudes of the hoop strains are larger than those of the axial strains at each *w*/*D*. This means that the soil inside the SPW is subjected to large horizontal stresses by the existence of SPW. It is reasonable from the comparison of Figs. 20 and 21 that-the foundation at step No. 7 has the resistance larger than that of the initial stage due to the contact of the raft on the ground.

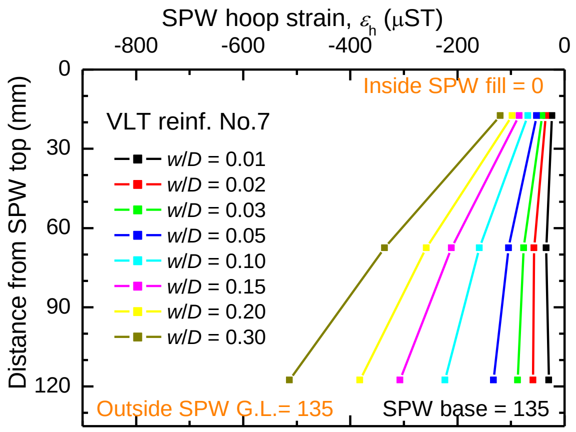

Fig. 22 SPW hoop strain distributions in the final reinforcement stage of VLTs on 4-pile pile foundation

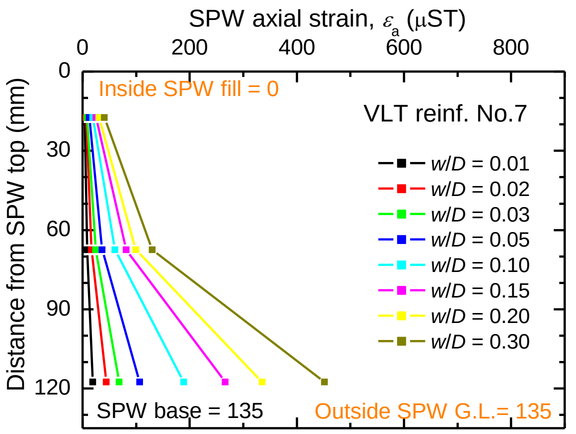

Fig. 23 SPW axial strain distributions in the final reinforcement stage of VLTs on 4-pile pile foundation

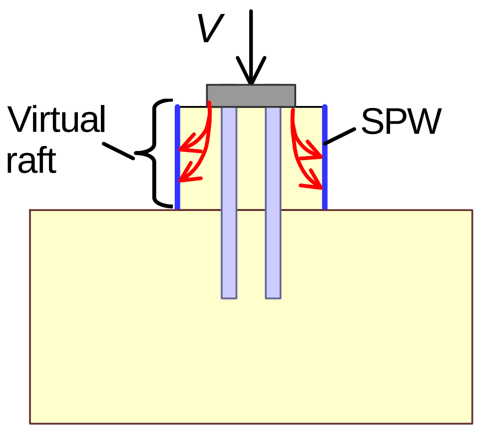

Fig. 24 Conceptual expression of stress transfer from the raft to the soil inside the SPW

Fig. 24 shows a conceptual expression of stress transfer from the raft base to the soil inside the SPW. A part of the vertical load on the foundation is supported by the raft. The vertical stresses at the raft base are transferred to the soil inside the SPW. The horizontal stresses as well as vertical stress in the soil are increased by the increase in the raft base stresses owing to the existence of the SPW.

Hence, it seems to be reasonable the raft resistance after the construction of the SPW becomes larger than that in the initial condition. It is inferred from the experimental results that efficiency of the SPW reinforcement is governed by size relative to the existing foundation and stiffness of the SPW as well as stiffness of the soil inside the SPW.

4. Concluding remarks

From the experimental results of model load tests on single pile and 4-pile pile foundation, it was demonstrated that the method of SPW reinforcement is very efficient and promising. On the other hand, numerical analyses of some actual pile foundations which have potential risks of settlement and collapse in Thailand should be carried out to find efficient configurations of the sheet pile wall reinforcement. Finally, in order to investigate the influences of flood load and scouring, and to validate the proposed reinforcing method, a full scale field test should be carried out.

The reinforcement mechanism of the SPW method mentioned above was confirmed through numerical analyses of the experiments by Tikanta et al (2017).

References

Fukada, H., Kato, K., Aoyagi, M., Inagawa, H and Shioi, Y. 2005. Application of Reinforcing Methods for Existing Pile Foundation on Soft Ground (In-cap Method). Public Works Research Institute: The 23rd US - Japan Bridge Engineering Workshop. Retrieved July 1, 2014 (www.pwri.go.jp/eng/ujnr/tc/g/pdf/23/23-7-3kato.pdf)

Tikanta, T., Matsumoto, T., Vu, A.T., Kobayashi, S., Shimono, S. and Bamrungwong, C. 2017. Fundamental experiments on a reinforcement method using sheet pile wall for bridge pile foundations subjected to pile embedment reduction and numerical validation, Geotechnical Engineering Journal of the SEAGS & AGSSEA, Vol. 48, No. 3, pp. 26-39.